Deletion of the E3-6.7K/gp19K region reduces the persistence of wild type adenovirus in a permissive tumor model in Syrian hamsters.

Sergia Bortolanza PhD[1], Maria Bunuales BSc[1], Pilar Alzuguren BSc[1], Oscar Lamas PhD[1], Rafael Aldabe PhD[1], Jesus Prieto MD PhD[1,2], Ruben Hernandez-Alcoceba MD PhD[1].

1. Division of Hepatology and Gene Therapy, CIMA. Foundation for Applied Medical Research. School of Medicine. University of Navarra. Pamplona, Spain.
2. CIBERehd. University Clinic. Navarra. Spain

Correspondence should be addressed to RHA (rubenh@unav.es)

Edificio CIMA. Av. Pio XII, 55

31008-Pamplona. Navarra, Spain

Phone +34-948194700

Fax +34-948194717

Running title: Persistence of E3-6.7K/gp19K-deleted adenoviruses

Keywords: E3 region; Oncolytic adenovirus; Syrian hamster; replication; luciferase.

Abstract

A partial deletion of the adenovirus E3 region, comprising the overlapping 6.7K/gp19K genes has been described for the incorporation of therapeutic genes in "armed" oncolytic adenoviruses. This deletion allows the insertion of up to 2.5 kb genetic material into the virus and ensures strong expression of transgenes without reducing the replication and cytolytic potency of viruses *in vitro*. E3-gp19K and 6.7K proteins are involved in avoiding recognition and elimination of infected cells by the host immune system. Therefore, we have studied the effect of this deletion on the replication and transgene expression of the virus in immunocompetent models based on Syrian hamsters. Tumors were established by intrahepatic injection of pancreatic cancer cells with moderate (HaP-T1, HP-1) or low (H2T) permissivity for adenovirus replication. The wild type human adenovirus 5 (Ad5) or a modified version containing the luciferase gene in the E3-6.7K/gp19K locus (Ad-WTLuc) were injected intratumorally. We found that elimination of Ad-WTLuc was faster than Ad5 in HaP-T1 and HP-1 tumors. In contrast, no differences were observed when the same tumor was established in severely immunocompromised NOD-scid IL2Rγ^{null} mice. In addition, virus-mediated luciferase expression was more stable in these animals. These results suggest that the lack of E3-6.7K/gp19K genes may accelerate the clearance of oncolytic adenoviruses in some immunocompetent tumor models.

Introduction

Experience accumulated in clinical trials on a variety of cancers with different oncolytic adenoviruses (conditionally replicative adenoviruses, CRAds) indicate that these agents are safe, but their efficacy as single agents is poor [1]. Strong physical and immunological barriers limit the biodistribution and cytolytic effect of the viruses and virtually abolish the robust antitumor effect demonstrated in animal models. Therefore, new mechanisms to enhance their efficacy are needed. The incorporation of therapeutic genes in the viruses could overcome some of their limitations and provide new mechanism of action with potential synergistic effects [2]. These genes include immunomodulatory agents, pro-drug converting enzymes and anti-angiogenic agents, among others. Adenovirus is a double-stranded linear DNA virus with a compact genome and relatively strict size constrains for encapsidation. Only an increase of up to 5% the original size is allowed without reducing the efficacy of genome packaging [3]. This determines that in many cases deletion of endogenous genes is needed in order to insert exogenous sequences such as long regulatory regions or transgenes. Partial or complete deletions of the E3 region in subgroup C human adenoviruses are commonly used, because this region is dispensable for viral growth *in vitro*. However, many genes involved in protection from antiviral responses are located in this region [4], and there is evidence indicating that restoration of E3 genes increases the oncolytic potency of adenoviruses *in vivo* [5]. The E3 region is a complex transcription unit in which a common promoter, alternative splicing and two polyadenylation signals (E3A and E3B) determine the expression of at least 7 different proteins [6]. Most of them work in coordination for avoiding recognition and destruction of infected cells by the immune system in early phases of the viral cycle [4]. Only the E3-11.6K protein (adenovirus death protein, ADP) has pro-apoptotic

functions, but its expression is stimulated by the major late promoter after replication has been completed, in order to facilitate release of virions from the cell [7]. The E3-10.4K/E3-14.5K proteins (receptor internalization and degradation, RID α,β complex) are involved in the destruction of death receptors such as Fas and tumor necrosis factor (TNF)-related apoptosis-inducing ligand (TRAIL) receptors 1 and 2, thus protecting infected cells from apoptosis induced by the immune system [8, 9]. The E3-14.7K protein also inhibits apoptosis induced by TNFα [10]. E3-6.7K collaborates with the RID complex in degradation of the TRAIL receptor 2 [11], and it inhibits apoptosis induced by Ca2+ release from the endoplasmic reticulum (ER) [12]. E3-gp19K inhibits the transport of major histocompatibility complex class I (MHC-I) molecules form the ER to the plasma membrane, thus reducing the display of viral peptides and avoiding the detection of infected cells by specific cytotoxic T lymphocytes [13]. Detailed studies of the E3 region have demonstrated that selective deletions can be used to insert exogenous genes without disrupting expression of adjacent E3 genes [14-16]. This is important, since some E3 proteins, such as ADP, are required for maintaining the cytolytic potency of the virus [17]. The use of endogenous promoter and polyadenylation signals reduces the requirement of exogenous genetic material and ensures strong expression of the transgenes. Following these principles, a 6.7K/gp19K deletion comprising nucleotides 28532 to 29355 in Ad5 genome has been successfully used for the insertion of therapeutic genes [16]. The E3-6.7K and gp19K genes are encoded by the same mRNA and have slightly overlapping open reading frames. Deleting both genes would allow the incorporation of foreign sequences up to 2.5 kb in length. However, the lack of these genes could accelerate the clearance of the virus and the infected cells *in vivo*, as observed for gp19K in mice [18]. On the other hand, these viral functions may be redundant for an oncolytic adenovirus if the target cells in the tumor have developed

analogous mechanisms to prevent apoptosis and recognition by the immune system. If this is the case, deletion of E3-6.7K and/or gp19K would increase the cancer specificity of the virus. However, elucidating the influence of E3 deletions on the performance of oncolytic adenoviruses has been traditionally hampered by the lack of immunocompetent tumor models in which human adenovirus can complete its viral cycle. More recently, the identification of several murine cancer cell lines with various degrees of permissivity for adenovirus replication made possible the initial studies in this subject [19]. Rapid clearance of viruses with extensive deletions including the RID complex and E3-14.7K genes was observed in these tumors, whereas a 152 bp deletion affecting only the gp19K gene caused no evident effect [20]. Unfortunately, this small deletion does not provide a significant increase in the cloning capacity of the virus, and the influence of placing a transgene in this location is unknown. In the present work we have constructed a vector based in the Ad5 genome in which the firefly luciferase is inserted in the E3-6.7K/gp19K locus (Ad-WTLuc vector). Using a recently described immunocompetent model based in Syrian hamsters [21], we have studied the persistence of replication for Ad-WTLuc versus Ad5, and the kinetics of luciferase expression of Ad-WTLuc after intratumor inoculation. Replication and spread of Ad5 and related CRAds has been previously demonstrated in Syrian hamsters [22, 23]. In our specific adaptation of the model, intrahepatic injection of hamster pancreatic cancer cells gives rise to a progressive tumor growth in the liver and extensive infiltration of surrounding tissues [21]. Cells with different *in vitro* permissivity for adenoviral replication have been used. We describe here that immunocompetent animals eliminate Ad-WTLuc faster than Ad5 in tumors derived from the most permissive cells. In contrast, when the same tumors were established in mice with severely impaired innate and adaptive immune system, no differences were observed and the expression of luciferase was stabilized.

These results suggest that elimination of the E3-6.7K/gp19K genes may accelerate the clearance of oncolytic adenoviruses in some immunocompetent hosts.

Materials and Methods

Cell lines and cultures.

The human cell lines HEK 293 (ATCC#CRL-1573), A549 (lung cancer, ATCC# CCL-185), HuH-7 (hepatocellular carcinoma, courtesy of. Dr. Brechot, INSERM, Paris, France), and the Syrian hamster pancreatic cancer cell lines H2T (courtesy of Dr. Townsend, University of Texas Medical Branch, TX, USA), HaP-T1 (German Collection of Micro organisms and Cell Culture, Cat. ACC 222) and HP-1 [24] (Courtesy of Dr. Hollingsworth, University of Nebraska Medical Center, Omaha NE, USA), were grown in DMEM supplemented with 10% FBS, 100 U/ml penicillin, 100μg/ml streptomycin and 2mM L-glutamine. All cells were maintained at 37°C with 5% CO_2 in a humidified incubator.

Virus construction and production.

Based on the previously described pSEHE2F plasmid [25], we applied standard subcloning techniques using intermediate plasmids to obtain a deletion of the E3-6.7K/gp19K region flaked by ClaI sites. The firefly luciferase gene from the pGL3-Basic plasmid (Promega) was inserted in this location using NarI sites to generate the pSEHE2F-Luc plasmid. In order to restore the wild type E1A and E4 regions, the 12.5 Kb NdeI fragment from pSEHE2F-Luc plasmid that includes the transgene, was introduced into the pTG3602 plasmid [26] encoding the genome of Ad5. The new plasmid was named pAd-Luc and contains a deletion of the E3-6.7K/gp19K region with insertion of the luciferase gene. In order to obtain a virus with the same E3 deletion but no transgene, we followed a parallel subcloning procedure. In this case the 6.7K/gp19K-deleted 12.5 Kb NdeI fragmente that was introduced in the pTG3602 plasmid lacked the luciferase gene, and the resulting plasmid was called pTG-DE3. The Ad-WTLuc and

Ad-DE3 viruses were obtained by transfection of the PacI-digested pAd-Luc and pTG-DE3 plasmids in 293 cells, respectively. After selection of individual clones, structure of the modified E3 region was verified by sequencing. The Ad5 virus was obtained from ATCC (Catalog number VR5). The Ad-CMVLuc virus was purchased from Vector Biolabs (Philadelphia, USA). All viruses were amplified in 293 cells and purified by ultracentrifugation in CsCl gradient. Quantification of infectious units (iu) was done using the Adeno-X rapid titer kit (Clontech)

Animal procedures.

Liver metastases of pancreatic cancer were established in Syrian (Golden) hamsters (*Mesocricetus Auratus*; *HSD HAN: AURA,* 5 weeks of age, Harlan, Barcelona, Spain) by intrahepatic injection of 2,5x10^6 H2T cells, 1x10^6 HaP-T1 cells or 2.5x10^6 HP-1 cells following laparotomy, as previously described [21]. Viruses were injected intratumorally 2 weeks after cell implantation of HaP-T1 and HP-1 cells, and 5weeks after implantation of H2T cells. Injection was performed in 50 µl total volume of saline solution. Tumor xenografts were induced in the flank of NOD-scid IL2Rγ^{null} mice [27] (NOD.Cg-*Prkdc*^{scid}Il2rg^{tm1Wjl}/SzJ, stock 005557, The Jackson Laboratory) by subcutaneous inoculation of 10^6 HaP-T1 cells. When tumors reached a volume of 300-500 mm^3 (V= (Dxd^2)/2, where D and d are the major and minor diameters, respectively), animals were treated subcutaneously with a single dose of 600 mg/kg methyl-prednisolone acetate (Sanofi-Aventis). Forty eight h later, viruses were injected intratumorally as described above. Animals were maintained under specific pathogen-free conditions and all procedures were carried out following protocols approved by the local ethical committee in accordance with recommendations for proper care and use of laboratory animals.

***In vivo* bioluminiscence detection.**

Ten minutes before luciferase detection, mice and hamsters received an intraperitoneal injection of 100 µl or 300 µl D-Luciferin Firefly (Xenogen), respectively. Animals were anesthesized by intraperitoneal injection of a mixture of ketamine and xylazine and placed in a dark chamber connected to a cooled charge-coupled device (CCD) camera (IVIS, Xenogen). Photon emission was quantified and analyzed using Living Image Software (Xenogen).

Luciferase assay in cell cultures.

Cells were seeded in 24-well plates with $3x10^4$ cells/well and were infected 24 h later with Ad5 or Ad-CMVLuc at MOI 1. The MOI (multiplicity of infection) is defined as the number of infectious units per cell (iu/cell). Viruses were removed 2 h later and then cells were washed once with PBS and incubated in DMEM supplemented with 2% FBS at 37°C. At different times post-infection, cells were lysed and analyzed for luciferase activity, using the Luciferase Assay System (Promega) as indicated by the manufacturer.

***In vitro* viral replication assay (virus burst size).**

Cells ($2x10^4$ /well) were cultured in 24-well plates overnight and infected with Ad5 and Ad-WTLuc in DMEM supplemented with 2% FBS. The MOI was adjusted for each cell line in order to obtain infection of more than 50% cells. Thus, HuH-7, HaP-T1, HP-1 and H2T cells were infected at MOI 50, and the A549 cell line was infected at MOI 25. Viruses were removed 2 h later and then cells were washed once with PBS and incubated in DMEM supplemented with 2% FBS at 37°C. Forty-eight hours later cells

were harvested, resuspended in PBS and lysed by three cycles of freezing and thawing. The amount of infective virus present in the cells was quantified by the Adeno X Rapid titer kit (BD Bioscience).

***In vitro* viability assays**. Cells were seeded in 96-well tissue culture plates at $5x10^3$cells/well and 24 h later they were infected with serial dilution of viruses. Cell viability was determined 5 days after infection by crystal violet staining. Briefly, cells were fixed for 10 min in 0,5% glutaraldehyde solution at room temperature, incubated for 30 min in 0,5% crystal violet solution (Sigma) and rinsed with water. Air-dried cells were solubilized with a 10% acetic acid solution and quantified by reading absorbance at 595 nm. Data were analyzed using the PrismGraphPad program.

Quantification of virus production *in vivo*.

At different times post-infection, tumors were frozen in liquid Nitrogen and 100-400 mg of tissue were homogenized in 1 ml of DMEM supplemented with 10% FBS. After 3 cycles of freezing and thawing, samples were centrifuged at 10,000 g for 5 minutes and viruses in the supernatant were quantified by the Adeno X Rapid titer kit (BD Bioscience).

RNA isolation and analysis of penton base expression by RT-PCR

Total RNA was extracted from tumor samples using TriReagent (Sigma) according to the manufacturer's instructions. Complementary DNA was synthesized from 2 μg RNA with M-MLV RT in the presence of RNase OUT (Invitrogen). For real-time PCR reaction, 5 μl of cDNA was incubated with specific primers for Adenovirus penton base gene (forward 5'-ACCTGGTGGACAACAAGTCA-3'; reverse 5'-

ACATTTGGCATGTTGGTAGGTGC-3') using a BioRad iQ iCycler Detection System (BioRad Laboratories, Ltd) with SYBR green fluorophore. For sample normalization, the hamster β-actin cDNA was amplified using the primers 5′-GTCGTACCACTGGCATTGTG-3′ (forward) and 5′-GTCACGCACAATTTCCCTCT-3′ (reverse). Values are represented by $2^{\Delta Ct}x10^4$, where ΔCt indicates the difference in the threshold cycle between β-actin and penton mRNAs.

DNA isolation and quantification of viral genomes.

DNA was extracted from tumor samples using the QIAmp DNA Mini Kit (Qiagen) according to the manufacturer's instructions. The abundance of viral copies was determined by quantitative PCR from 200 ng of DNA using primers specific for the E4 region: 5'-CTAACCAGCGTAGCCCA-3' (forward) and 5'-TGAGCAGCACCTTGCATTTT-3' (reverse). A BioRad iQ iCycler Detection System (BioRad Laboratories, Ltd) with SYBR green fluorophore sample was used. To calculate the amount of copies/μg, a standard curve of purified Ad5 genomes was prepared.

Statistical analysis.

Statistical comparisons were done using the Mann Whitney test (GraphPad Prism program, GraphPad Software).

Results

Characterization of the Ad-WTLuc virus *in vitro*.

The Ad-WTLuc virus is based on the Ad5 genome, in which a portion of the E3 region comprising the 6.7K/gp19K genes has been deleted (nucleotides 28555 to 29355), and the firefly luciferase gene has been inserted. Taking into consideration this 0.8 kb deletion, the insertion of the luciferase gene (1.7 kb in length) is not expected to compromise the packaging efficiency of the virus. As previously described [16], this modification did not alter the expression of contiguous E3 genes such as ADP (data not shown). In order to identify potential alterations in the properties of the virus, first we compared the progeny produced by Ad-WTLuc and the parental virus Ad5 in different cell lines (virus burst size). To this end, human cancer cell lines HuH-7, A549 and hamster pancreatic cancer cell lines HaP-T1, HP-1 and H2T were infected with the viruses, and the amount of infective viral particles produced in a single viral cycle was quantified (figure 1). As previously reported for Ad5, human cell lines were the most efficient viral producers (up to 10^3 infectious units per cell, iu/cell), followed by HaP-T1 (10^2 iu/cell). Although progressive viral amplification has been demonstrated in the H2T cells [21], virus yield was very low at 48 h, suggesting low permissivity and delayed viral cycle. Ad-WTLuc showed the same tendency as the parental virus, with a moderate reduction of virus production in some cell lines such as HuH-7, HaP-T1, HP-1 and H2T, and slight increase in A549 cells. We next investigated if these variations had an impact on the ability of the virus to cause cytopathic effect and death of infected cells, which is one of the main properties of oncolytic adenoviruses. The same cell lines described above were infected with different MOIs and maintained for 5 days, in order to evaluate the effect of virus amplification and spread. In figure 2 we show the

percentage of cells that survive at the end of the experiment, compared with non-infected controls. The results indicate that the cytolytic effect of Ad-WTLuc is not impaired in any of the cell lines studied.

Clearance of Ad-WTLuc is accelerated in HaP-T1 tumors established in immunocompetent hamsters, but not in severely immunocompromised mice.

We studied if the gene deletion/insertion introduced in the Ad-WTLuc affects the properties of the virus *in vivo*. Liver metastases of pancreatic cancer were established by intrahepatic injection of HaP-T1, HP-1 or H2T cells in immunocompetent Syrian hamsters. Once the tumors were evident (2 weeks after cell implantation for HaP-T1 and HP-1 and 5 weeks for H2T cells), $2x10^9$ iu of Ad-WTLuc or Ad5 were injected locally. Animals were sacrificed 2 or 4 days later, and the presence of infective viral particles was quantified in tissue homogenates from the different tumors. Two days after infection, it is possible that some viruses recovered from tumors correspond to particles retained in the tissues from the original injection, before they have infected and replicated in the cells. By comparison with a replication-deficient adenoviral vector, we determined that this represents less than 10% of viable viruses. Therefore the percentage of residual virus from the original input is low, and it is reduced over time. In fact, if a replication-deficient adenoviral vector is injected, no viable viruses can be recovered from HaP-T1 tumors at day 4 [21]. In figures 3A and 3B we show that, as previously described, viral production of Ad5 was not different in HaP-T1 and H2T cells *in vivo* [21]. In both cases, a drop in virus content was observed from day 2 to day 4, but progeny production of the wid-type virus could still be detected at the latter time point. The rapid decrease in Ad5 production evidences the strong control that the innate immune system exerts on virus amplification and spread. In the case of Ad-WTLuc, a moderate

reduction in virus yield versus Ad5 was present already at day 2 in HaP-T1 and H2T tumors, probably reflecting the lower virus burst size observed *in vitro*. The main finding, however, was the rapid neutralization of Ad-WTLuc from HaP-T1 tumors (figure 3B). Virtually no infective particles could be recovered from these tumors at day 4. The same result was obtained with HP-1 tumors (figure 3C). Since the sensitivity of this *in vivo* assay is low, we cannot rule out the possibility that small amounts of viruses are produced, but in any case the difference with Ad5 is evident. In contrast, production of Ad-WTLuc and Ad5 showed a similar tendency in H2T tumors (figure 3A). To demonstrate that the presence of the luciferase gene in the Ad-WTLuc virus is not responsible for its rapid clearance in HaP-T1 cells, we repeated the same experiment with a virus that presents the same 6.7K/gp19K deletion, but carries no transgene (Ad-DE3). As shown in figure 3B, a rapid elimination of Ad-DE3 was also observed.

We next studied other indicators of viral activity in samples from HaP-T1 and H2T tumors in order to confirm the preferential neutralization of Ad-WTLuc in HaP-T1 tumors. Active viral cycle was determined by analysis of late gene transcription. RNA was extracted from tumor samples and the mRNA corresponding to the L5-polypeptide III (which forms the penton base protein) was quantified by qRT-PCR (figure 4). A reduction of mRNA copies from day 2 to day 4 was observed in all cases, suggesting that viral activity is being controlled. However, blockade of Ad-WTLuc was significantly stronger than Ad5 in HaP-T1 tumors, in agreement with the previous results. Persistence of viral genomes was also determined in tumor samples from day 4, using qPCR for detection of the E4 gene (figure 5). Although we found great variability among different animals, a reduction of copy numbers was observed in HaP-T1 tumors treated with Ad-WTLuc, compared with Ad5. Together with the absence of viable

viruses recovered from these tumors, our data indicate that the spread of the virus is being rapidly blocked.

In order to determine if the immune system is responsible for this phenomenon, we compared the persistence of Ad5 and Ad-WTLuc in a HaP-T1 xenograft model established on severely immunosuppressed mice. NOD-scid IL2Rγ^{null} mice lacking B, T and NK cells [27], were inoculated subcutaneously with HaP-T1 cells in order to avoid open surgery and deep anesthesia in these animals. Once tumors were established (approximately 2 weeks after inoculation), mice were treated with a single intraperitoneal dose of methyl-prednisolone acetate (MPA) in order to further decrease the number and function of the remaining leukocytes, such as macrophages [28]. Forty eight hours after MPA injections, $5x10^8$ iu of Ad5 or Ad-WTLuc were inoculated intratumorally, and animals were sacrificed 4 days later. An equal dose of the replication-deficient Ad-CMVLuc virus [21] was inoculated in a third group of animals to assess the replication-independent persistance of adenovirus in the context of immunocompromised mice. In figure 6 A we show the quantification of viable viruses recovered from the tumors. No differences between Ad5 and Ad-WTLuc were detected, suggesting that both viruses can replicate equally well under these circumstances. In addition, equivalent gene expression (penton base) and genome copy numbers were detected in these tumors (figure 6B). These results indicate that abrogation of the immune system avoids the rapid clearance of Ad-WTLuc in HaP-T1 tumors. Interestingly, some viable viruses were recovered from Ad-CMVLuc-treated mice (figure 6A). Altough the amount is significantly lower than in the case of replication-competent viruses, Ad-CMVLuc was detected in all the animals. This is in contrast with data obtained in hamsters [21], and suggests that a small percentage of the original input

of virions remains intact in the tumor mass without infecting any cell, and can be extracted 4 days after inoculation in immunodeficient mice.

Viral replication and host immune responses limit the duration of transgene expression mediated by Ad-WTLuc.

Expression of transgenes inserted into the E3-6.7K/gp19K region of adenovirus is activated following the viral cycle [16], and is further amplified by the progressive increase in copy number. After lysis of the infected cells, persistence of expression will depend on the efficacy of virus spread. Culture of homogeneous cell populations *in vitro* favors infection of neighboring cells by the new viral progeny and allows progressive increase in luciferase expression. In figure 7A we show this phenomenon in HaP-T1 cells infected with a low MOI of Ad-WTLuc. As a negative control for replication, we used in parallel the Ad-CMVLuc vector, in which expression of luciferase is controlled by a CMV promoter. As early as 24 h post- infection, when the genomes of the input viruses have been replicated, lysates from cells infected with Ad-WTLuc presented high luciferase activity. In subsequent days, the activity was increased despite the cytopathic effect observed in a proportion of cells in the monolayer. In contrast, luciferase expression mediated by Ad-CMVLuc remained several orders of magnitude lower than the replicative virus during all the observation period. In order to study the effect of physical and immunological barriers on transgene expression, we injected $2x10^9$ iu of Ad-WTLuc or Ad-CMVLuc in HaP-T1 tumors established in the liver of Syrian hamsters. In figure 7B we represent the *in vivo* luciferase activity detected in the tumors over time, as an indicator of transgene expression. Day 1 refers to measurement 24 h after virus injection. As expected, the replication-competent virus achieved higher (at least 100-fold) activity than the conventional vector at early time points, probably reflecting the progression of viral

cycle in the cells infected by the injected virus. However, luciferase activity in Ad-WTLuc-infected tumors showed a sharp decline in subsequent days, with 4% activity at day 3; 0,5% at day 7 and levels close to baseline at day 10. In order to elucidate the role of the immune system in this rapid inhibition, we injected Ad-WTLuc in HaP-T1 tumors established in the NOD-scid IL2Rγ^{null} mice treated with corticoids. Absolute values of luciferase activity cannot be compared, since the dose of virus administered to mice was lower than in hamsters ($2x10^8$ iu) in order to avoid toxicity. However, comparing the kinetics of luciferase activity in both types of animals (figure 7C) reveals a clear stabilization of transgene expression in immunodeficient mice. The percentage of luciferase activity is represented for each group of animals, considering 100% the values obtained at day 1 after infection. In contrast with the rapid inhibition in hamsters, we observed a small increase at day 2 in NOD-scid IL2Rγ^{null} mice, and a gradual decrease in subsequent days, with maintenance of close to 20% activity at day 10 and approximately 3% at the end of the observation period (day 14). Animals were then sacrificed due to progression of tumor growth.

Discussion

The incorporation of therapeutic genes into CRAds generates vectors with complex mechanisms of action. The genomic modifications required for insertion and expression of exogenous material may alter the properties of the viruses at different levels, and understanding these changes is needed to design an efficient therapeutic strategy. *In vivo*, the role of the immune system is crucial, especially if alterations in the E3 region have been introduced. Selective deletions in the E3-6.7K/gp19K have been described to avoid major disruption of other genes in the E3 region and achieve efficient transgene expression *in vitro* [16]. Here we have verified that insertion of a luciferase gene in this location in the context of a wild type Ad5 genome does not impair significantly the capacity of the virus to replicate and induce cytopathic effect. By direct comparison with Ad5, some variations were observed in virus burst size, but they seem to be cell type-specific. For the *in vivo* studies, we have used for the first time the Syrian hamster model, which allows replication of Ad5 in tumors and other organs in the context of an immunocompetent host [21, 22]. As expected, development of an efficient adaptive immune response against adenovirus after a first exposure, with high titers of neutralizing antibodies and protection from virus re-administration was observed in these animals (data not shown). But in the present work we have focused on early events taking place few days after virus administration, when the innate immunity blocks the spread of replicative agents. The major finding in this study was the rapid inhibition of Ad-WTLuc production compared with the parental Ad5 virus in tumors derived from cells with moderate permissivity for adenovirus replication (HaP-T1 and HP-1). The functional neutralization of Ad-WTLuc 4 days after infection was confirmed by analysis of other parameters such as reduction of late viral gene transcription and copy numbers in tumor samples. This effect is mediated by the innate immune system,

since no difference in virus persistence was observed in NOD-scid IL2Rγ^{null} mice treated with corticoids, at least in the short term. These mice lack functional T and B and cells due to the *scid* mutation; are devoid of NK cells and present dendritic cell dysfunctions due to a deletion in the IL2Rγ gene. In addition, they suffer alterations in complement activity and macrophage function derived from the NOD background [27, 29]. In our experiments, residual activity of the immune system was transiently inhibited by corticoid treatment. Under these circumstances, most immunological barriers for virus amplification and spread should be impaired. In fact, using bioluminescence as a surrogate marker for Ad-WTLuc activity, we observed a clear difference between Syrian hamsters and NOD-scid IL2Rγ^{null} mice harboring HaP-T1 tumors. Transgene expression was rapidly inhibited in hamsters, with less than 1% luciferase signal detectable one week after injection. In contrast, NOD-scid IL2Rγ^{null} mice retained approximately 20% activity at this time point. However, it is important to note that the activity of Ad-WTLuc was also restricted in immunodeficient mice, with only an early and brief increase in expression followed by a progressive decline. This differs from the intrinsic capacity of the virus to propagate *in vitro*. These data indicate that, apart from the cellular components of the innate immune system, other factors limit the amplification of adenovirus in the microenvironment of the tumor. It seems that the balance between viral replication, cytopathic effect and infection of neighboring cells in the tumor results in a progressive loss of transgene expression that is accelerated by the immune system. It has been recently described that immunosuppression of Syrian hamsters using high dose cyclophosphamide enhances the replication of Ad5 in tumors and other organs [30]. However, differences in viral persistence were only observed at late time points, and not 3 or even 9 days after infection. In agreement with these results, when we treated hamsters bearing HaP-T1 tumors with cyclophosphamide, we could

not detect any increase in the amount of Ad5 or Ad-WTLuc virus recovered from tumors 4 days after infection (data not shown). This suggests that efficient abrogation of the early response against adenovirus will be difficult in immunocompetent hosts.

Detailed investigation of the mechanisms responsible for the rapid blockade of Ad-WTLuc replication in HaP-T1 and HP-1 tumors is in progress, and awaits development of suitable tools for immunological studies in hamsters. It has been reported that a small deletion affecting only the E3-gp19K gene causes no attenuation of adenovirus in an immunocompetent murine model [20]. This observation favors the hypothesis that the E3-6.7K deficiency is mostly responsible for the effect observed in our model. However, *in vitro* analysis performed so far have not demonstrated differences in the susceptibility to TNF receptor superfamily-induced apoptosis in HaP-T1 and H2T cells infected with Ad5 or Ad-WTLuc (data not shown). It also remains unclear why the accelerated inactivation of Ad-WTLuc in HaP-T1 and HP-1 is not observed in hamsters harboring H2T tumors. One possibility is the delayed replication and cytopathic effect observed in H2T cells, which may translate into an attenuated immune response *in vivo*. This could also account for the relatively high viral progeny production observed in this tumors compared with the *in vitro* data. In summary, we describe that the E3-6.7K/gp19K deletion may accelerate the blockade of replication-competent adenoviruses by the immune system in tumors derived from permissive cells. No alterations in other viral functions were detected, and early transgene expression was superior to first-generation adenoviruses. Therefore, this location may be adequate for the insertion of transgenes that require intense and short-term expression *in vivo*, such as vaccination and other immunogene therapy strategies against cancer.

Acknowledgements

We thank financial support from the Spanish Department of Education and Science (Grant SAF2003-08385 and SAF2006-04755). This project was founded in part by the UTE project CIMA. RHA is a recipient of Ramon y Cajal research contract from the Spanish Department of Education and Science. We are grateful to Drs. Brechot, Townsend, Hollingsworth and Alemany for providing cancer cell lines.

References

1 Aghi M and Martuza RL. Oncolytic viral therapies - the clinical experience. *Oncogene* 2005; **24**: 7802-16

2 Hermiston TW and Kuhn I. Armed therapeutic viruses: strategies and challenges to arming oncolytic viruses with therapeutic genes. *Cancer Gene Ther* 2002; **9**: 1022-35

3 Bett AJ, Prevec L and Graham FL. Packaging capacity and stability of human adenovirus type 5 vectors. *J Virol* 1993; **67**: 5911-21

4 Horwitz MS. Function of adenovirus E3 proteins and their interactions with immunoregulatory cell proteins. *J Gene Med* 2004; **6 Suppl 1**: S172-83

5 Zhu M, Bristol JA, Xie Y, Mina M, Ji H, Forry-Schaudies S, et al. Linked tumor-selective virus replication and transgene expression from E3-containing oncolytic adenoviruses. *J Virol* 2005; **79**: 5455-65

6 Wold WS, Tollefson AE and Hermiston TW. E3 transcription unit of adenovirus. *Curr Top Microbiol Immunol* 1995; **199 (Pt 1)**: 237-74

7 Tollefson AE, Scaria A, Hermiston TW, Ryerse JS, Wold LJ and Wold WS. The adenovirus death protein (E3-11.6K) is required at very late stages of infection for efficient cell lysis and release of adenovirus from infected cells. *J Virol* 1996; **70**: 2296-306

8 Shisler J, Yang C, Walter B, Ware CF and Gooding LR. The adenovirus E3-10.4K/14.5K complex mediates loss of cell surface Fas (CD95) and resistance to Fas-induced apoptosis. *J Virol* 1997; **71**: 8299-306

9 Benedict CA, Norris PS, Prigozy TI, Bodmer JL, Mahr JA, Garnett CT, et al. Three adenovirus E3 proteins cooperate to evade apoptosis by tumor necrosis factor-related apoptosis-inducing ligand receptor-1 and -2. *J Biol Chem* 2001; **276**: 3270-8

10 Krajcsi P, Dimitrov T, Hermiston TW, Tollefson AE, Ranheim TS, Vande Pol SB, et al. The adenovirus E3-14.7K protein and the E3-10.4K/14.5K complex of proteins, which independently inhibit tumor necrosis factor (TNF)-induced apoptosis, also independently inhibit TNF-induced release of arachidonic acid. *J Virol* 1996; **70**: 4904-13

11 Lichtenstein DL, Doronin K, Toth K, Kuppuswamy M, Wold WS and Tollefson AE. Adenovirus E3-6.7K protein is required in conjunction with the E3-RID protein complex for the internalization and degradation of TRAIL receptor 2. *J Virol* 2004; **78**: 12297-307

12 Moise AR, Grant JR, Vitalis TZ and Jefferies WA. Adenovirus E3-6.7K maintains calcium homeostasis and prevents apoptosis and arachidonic acid release. *J Virol* 2002; **76**: 1578-87

13 Burgert HG, Maryanski JL and Kvist S. "E3/19K" protein of adenovirus type 2 inhibits lysis of cytolytic T lymphocytes by blocking cell-surface expression of histocompatibility class I antigens. *Proc Natl Acad Sci U S A* 1987; **84**: 1356-60

14 Hawkins LK and Hermiston T. Gene delivery from the E3 region of replicating human adenovirus: evaluation of the E3B region. *Gene Ther* 2001; **8**: 1142-8

15 Hawkins LK and Hermiston TW. Gene delivery from the E3 region of replicating human adenovirus: evaluation of the ADP region. *Gene Ther* 2001; **8**: 1132-41

16 Hawkins LK, Johnson L, Bauzon M, Nye JA, Castro D, Kitzes GA, et al. Gene delivery from the E3 region of replicating human adenovirus: evaluation of the 6.7 K/gp19 K region. *Gene Ther* 2001; **8**: 1123-31

17 Tollefson AE, Scaria A, Ying B and Wold WS. Mutations within the ADP (E3-11.6K) protein alter processing and localization of ADP and the kinetics of cell lysis of adenovirus-infected cells. *J Virol* 2003; **77**: 7764-78

18 Bruder JT, Jie T, McVey DL and Kovesdi I. Expression of gp19K increases the persistence of transgene expression from an adenovirus vector in the mouse lung and liver. *J Virol* 1997; **71**: 7623-8

19 Hallden G, Hill R, Wang Y, Anand A, Liu TC, Lemoine NR, et al. Novel immunocompetent murine tumor models for the assessment of replication-competent oncolytic adenovirus efficacy. *Mol Ther* 2003; **8**: 412-24

20 Wang Y, Hallden G, Hill R, Anand A, Liu TC, Francis J, et al. E3 gene manipulations affect oncolytic adenovirus activity in immunocompetent tumor models. *Nat Biotechnol* 2003; **21**: 1328-35

21 Bortolanza S, Alzuguren P, Bunuales M, Qian C, Prieto J and Hernandez-Alcoceba R. Human adenovirus replicates in immunocompetent models of pancreatic cancer in Syrian hamsters. *Hum Gene Ther* 2007; **18**: 681-90

22 Thomas MA, Spencer JF, La Regina MC, Dhar D, Tollefson AE, Toth K, et al. Syrian hamster as a permissive immunocompetent animal model for the study of oncolytic adenovirus vectors. *Cancer Res* 2006; **66**: 1270-6

23 Hjorth RN, Bonde GM, Pierzchala WA, Vernon SK, Wiener FP, Levner MH, et al. A new hamster model for adenoviral vaccination. *Arch Virol* 1988; **100**: 279-83

24 Batra SK, Metzgar RS, Worlock AJ and Hollingsworth MA. Expression of the human MUC1 mucin cDNA in a hamster pancreatic tumor cell line HP-1. *Int J Pancreatol* 1992; **12**: 271-83

25 Hernandez-Alcoceba R, Pihalja M, Qian D and Clarke MF. New oncolytic adenoviruses with hypoxia- and estrogen receptor-regulated replication. *Hum Gene Ther* 2002; **13**: 1737-50

26 Chartier C, Degryse E, Gantzer M, Dieterle A, Pavirani A and Mehtali M. Efficient generation of recombinant adenovirus vectors by homologous recombination in Escherichia coli. *J Virol* 1996; **70**: 4805-10

27 Shultz LD, Lyons BL, Burzenski LM, Gott B, Chen X, Chaleff S, et al. Human lymphoid and myeloid cell development in NOD/LtSz-scid IL2R gamma null mice engrafted with mobilized human hemopoietic stem cells. *J Immunol* 2005; **174**: 6477-89

28 Miller TA and Schaefer FW, 3rd. Characterization of a single dose methylprednisolone acetate immune suppression model using Cryptosporidium muris and Cryptosporidium parvum. *Vet Parasitol* 2006; **141**: 66-83

29 Ito M KK, Nakahata T. NOD/Shi-scid IL2rg null (NOG) mice more appropriate for humanized mouse models. *Journal* 2008; **324**: 53-76

30 Thomas MA, Spencer JF, Toth K, Sagartz JE, Phillips NJ and Wold WS. Immunosuppression enhances oncolytic adenovirus replication and antitumor efficacy in the Syrian hamster model. *Mol Ther* 2008; **16**: 1665-73

Figure legends

Figure 1. **Replication of Ad5 and Ad-WTLuc in *in vitro*.** Cancer cells from human (HuH-7, A549) and hamster (HaP-T1, H2T, HP-1) origin were infected for 2 h with Ad5 (white columns) or Ad-WTLuc (black columns) at the following MOIs: 50 for HuH-7, HaP-T1, HP-1 and H2T, and 25 for A549. Two days later cells were harvested and lysed. The amount of viable virions was quantified and is represented as iu/cell.

Figure 2. Cytolytic effect of viruses. HuH-7 (A), A549 (B), H2T (C), HaP-T1 (D) and HP-1 cells (E) were infected with Ad5 (squares, black line) or Ad-WTLuc (triangles, dotted line) at the indicated MOIs and cultured for 5 days. Viable cells were stained by crystal violet and the percentage of surviving cells versus non-infected controls is represented as a sigmoidal dose-response curve. Note the different scale in the X axis among the cell lines.

Figure 3. Viral production in tumors established in hamsters. Liver metastases of pancreatic cancer were established in Syrian hamsters by intrahepatic injection of H2T (A) HaP-T1 (B) or HP-1 (C) cells. After 2 weeks (HaP-T1, HP-1) or 4 weeks (H2T), hamsters were inoculated intratumorally with $2x10^9$ iu of different viruses: Ad5 (squares); Ad-WTLuc (triangles); or Ad-DE3 (circles). At the indicated times after infection, at lease 4 animals from each group were sacrificed. Tumors were lysed for determination of viable viral particles and represented as iu/mg tumor for each animal. *p<0,05 **p<0,01

Figure 4. Viral gene expression in tumors established in hamsters. Ad5 (white colums) or Ad-WTLuc (black colums) were inoculated intratumorally at $2x10^9$

iu/animal in tumors derived from HaP-T1 or H2T cells in the liver of Syrian hamsters. Groups of animals were sacrificed 2 or 4 days after infection, and RNA was extracted from tumors. Quantification of penton base mRNA was performed by qRT-PCR. Values are expressed as $2^{\Delta Ct}x10^4$, where ΔCt indicates the difference in the threshold cycle between β-actin and penton genes. *p<0,05 ***p<0,0001

Figure 5. Persistence of viral genomes in tumors established in hamsters. Ad5 (squares) or Ad-WTLuc (triangles) were inoculated intratumorally at $2x10^9$ iu/animal in tumors derived from HaP-T1 or H2T cells in the liver of Syrian hamsters. DNA was isolated from tumors collected 4 days after infection, and the amount of viral copies was determined by qPCR using primers specific for the E4 region. Values correspond to the number of viral copies/μg of DNA for each animal. *p<0,05.

Figure 6. Viral production and persistence of viruses in HaP-T1 tumors established in immunodeficient mice. Tumor xenografts were induced in the flank of NOD-scid IL2Rγ^{null} mice by subcutaneous inoculation of HaP-T1 cells. When tumors reached at least 300 mm^3 volume, animals received a single dose of 600mg/Kg of methylprednisolone, and 48 h later Ad5 (squares), Ad-WTLuc (triangles) or Ad-CMVLuc (circles) were injected intratumorally at $5x10^8$ iu/mouse. Four days later, animals were sacrificed and tumors were collected. (A) Viable viral particles were determined for each tumor and represented as iu/mg. (B) Quantification of penton base mRNA was performed by qRT-PCR (left pair of columns). Values are expressed as $2^{\Delta Ct}x10^4$ in the left Y axis, where ΔCt indicates the difference in the threshold cycle between β-actin and penton genes. The amount of viral copies was determined by qPCR

using primers specific for the E4 region (right pair of columns). Values in the right Y axis correspond to the number of viral copies/μg of DNA for each animal.

Figure 7. Transgene expression of Ad-WTLuc *in vitro* and *in vivo*. (A) HaP-T1 cells were infected with Ad-WTLuc (black columns) or Ad-CMVLuc (grey columns) at a MOI of 1. Cells were collected at different times post-infection, and luciferase activity was measured. Values correspond to luciferase units/μg protein. (B) A single dose of $2x10^9$ iu Ad-WTLuc (black columns) or Ad-CMVLuc (grey columns) was injected in HaP-T1 tumors established in the liver of Syrian hamsters. *In vivo* luciferase activity was analyzed over time and represented as photons/sec. (C) A single dose of $2x10^8$ iu Ad-WTLuc was injected in subcutaneous HaP-T1 tumors established in methyl-prednisolone-treated NOD-scid IL2Rγ^{null} mice. The evolution of *in vivo* luciferase activity was monitored and represented as percentage from day 1 after infection (black squares). Initial luminescence was $3x10^8$ photons/sec. Kinetics of luciferase activity in hamsters described in panel B are included as comparison (black triangles).

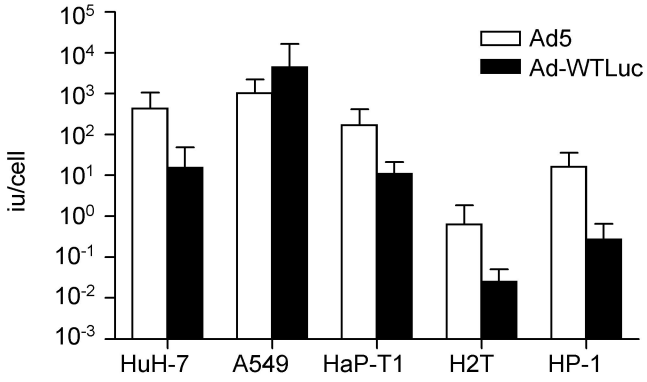
Ad5
Ad-WTLuc
iu/cell
10^5
10^4
10^3
10^2
10^1
10^0
10^{-1}
10^{-2}
10^{-3}
HuH-7
A549
HaP-T1
H2T
HP-1

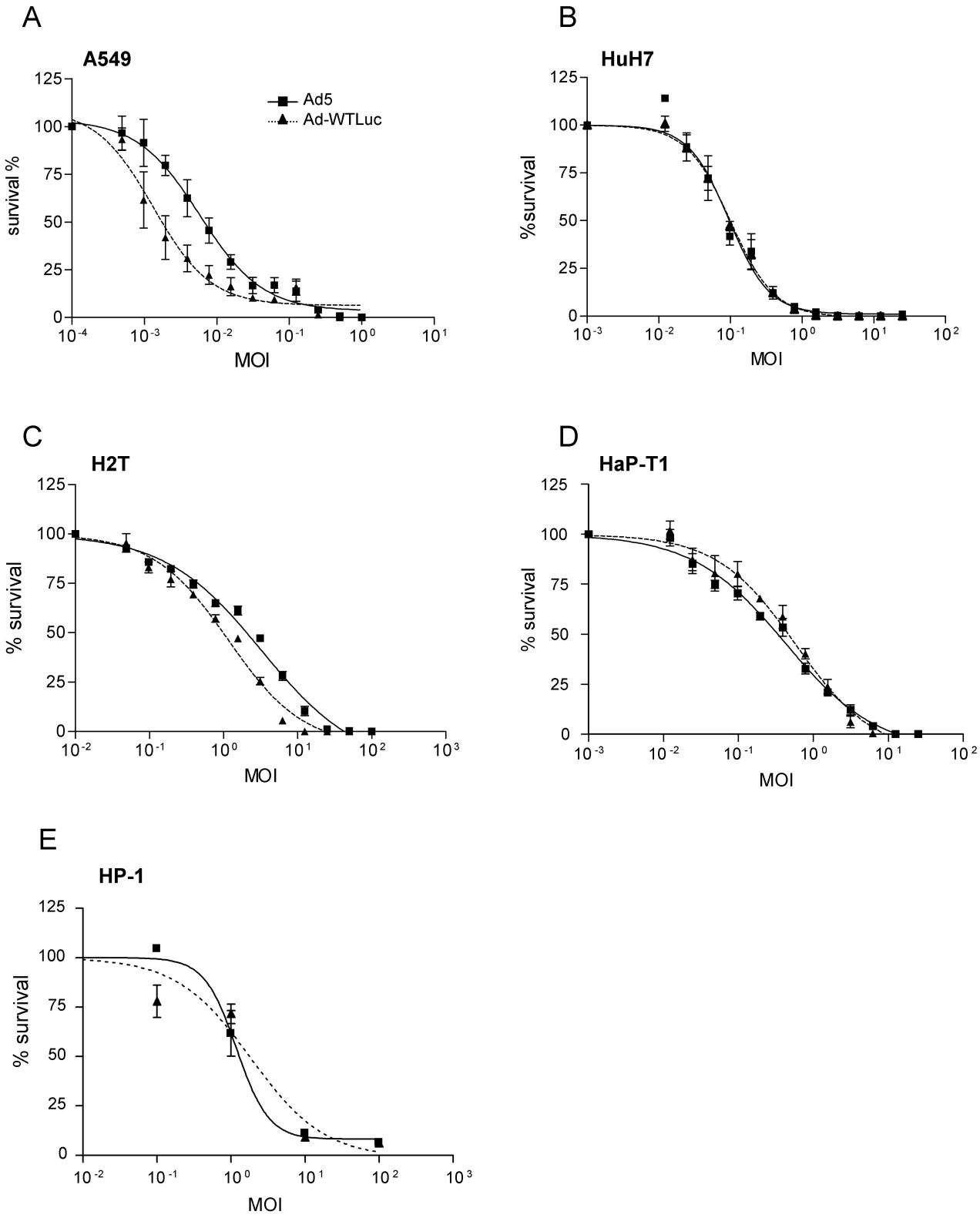
A
A549
Ad5
Ad-WTLuc
survival %
MOI
B
HuH7
%survival
MOI
C
H2T
% survival
MOI
D
HaP-T1
% survival
MOI
E
HP-1
% survival
MOI

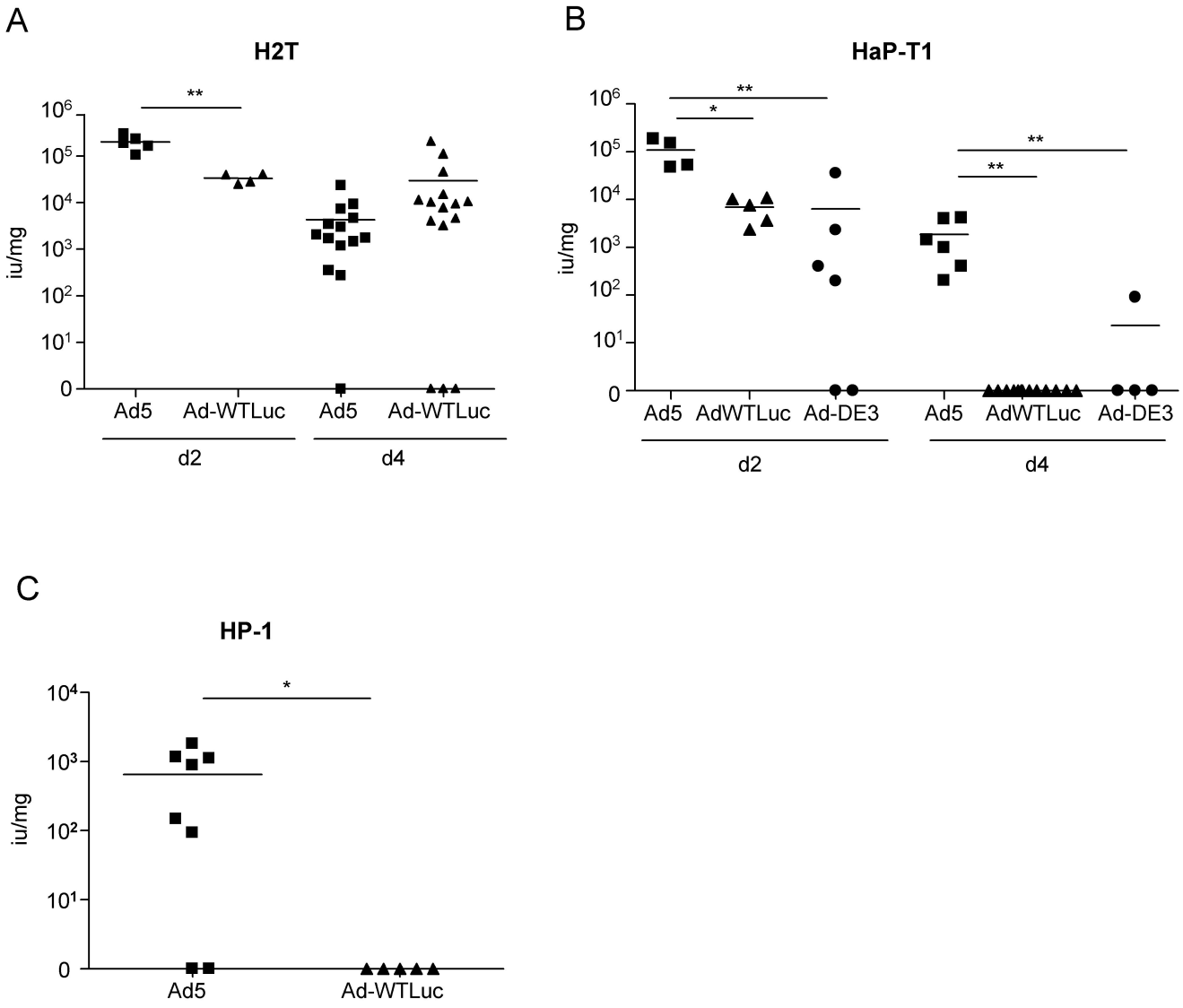
A
H2T
**
10^6
10^5
10^4
10^3
10^2
10^1
0
iu/mg
Ad5
Ad-WTLuc
Ad5
Ad-WTLuc
d2
d4
B
HaP-T1
**
*
**
**
10^6
10^5
10^4
10^3
10^2
10^1
0
iu/mg
Ad5
AdWTLuc
Ad-DE3
Ad5
AdWTLuc
Ad-DE3
d2
d4
C
HP-1
*
10^4
10^3
10^2
10^1
0
iu/mg
Ad5
Ad-WTLuc

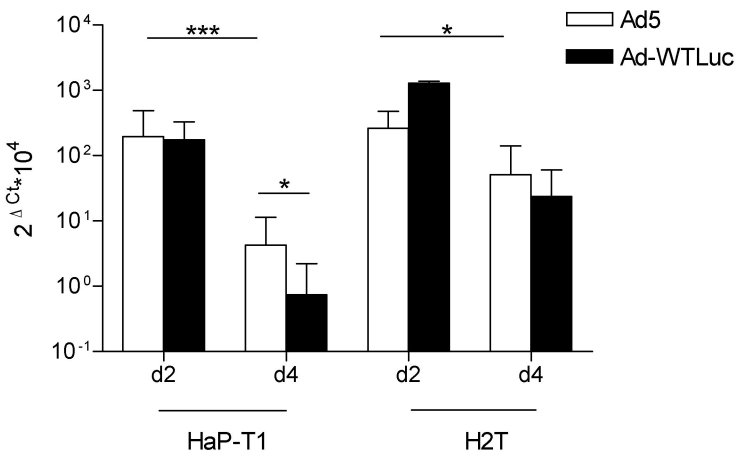
Ad5
Ad-WTLuc
10^4
10^3
10^2
10^1
10^0
10^{-1}
$2^{\Delta Ct}*10^4$
***
*
*
d2
d4
d2
d4
HaP-T1
H2T

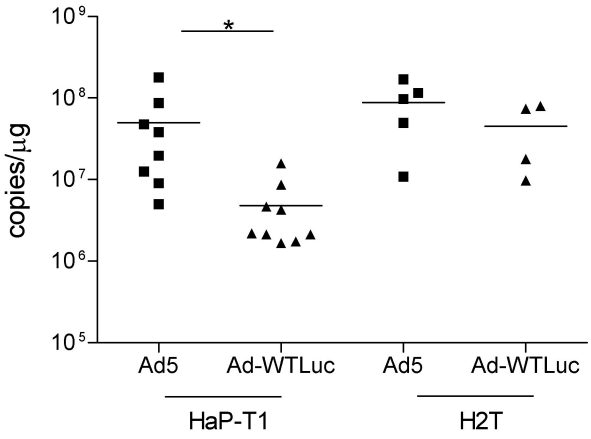
10^9
10^8
10^7
10^6
10^5
copies/μg
*
Ad5
Ad-WTLuc
Ad5
Ad-WTLuc
HaP-T1
H2T

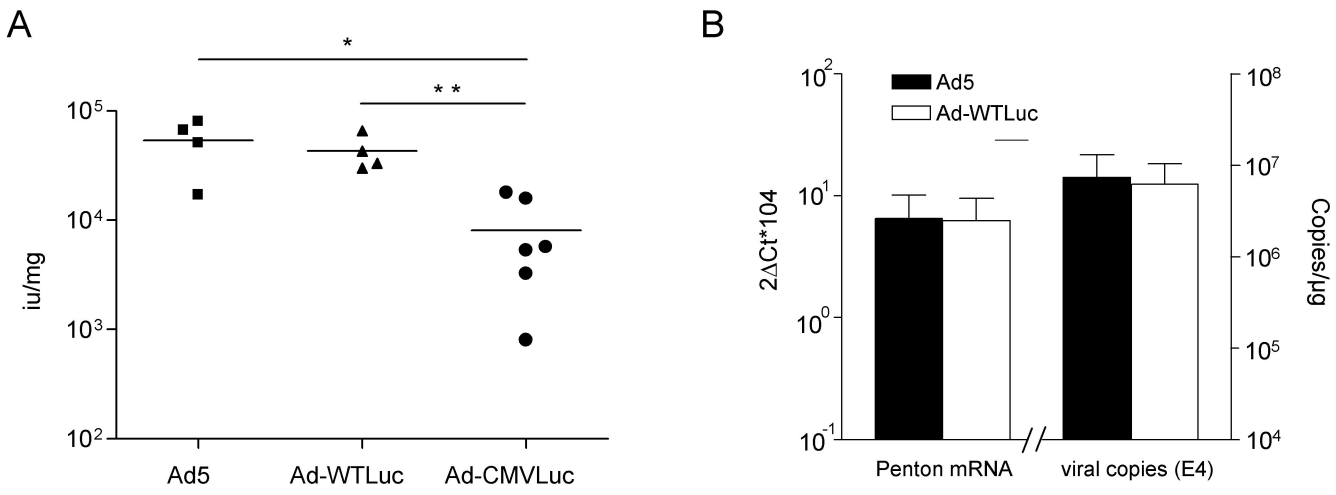
A
*
* *
iu/mg
10^5
10^4
10^3
10^2
Ad5
Ad-WTLuc
Ad-CMVLuc
B
Ad5
Ad-WTLuc
2ΔCt*104
Copies/µg
10^2
10^1
10^0
10^-1
10^8
10^7
10^6
10^5
10^4
Penton mRNA
viral copies (E4)

A

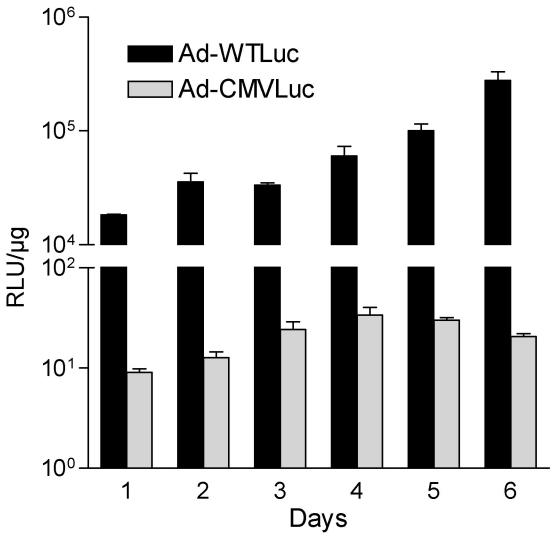
Ad-WTLuc
Ad-CMVLuc
RLU/µg
Days

B

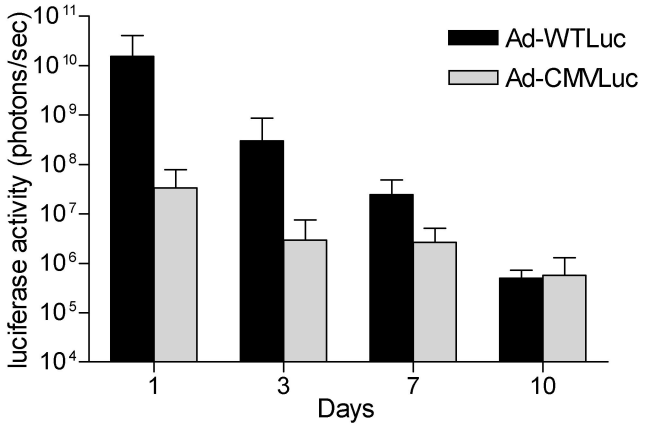
Ad-WTLuc
Ad-CMVLuc
luciferase activity (photons/sec)
Days

C

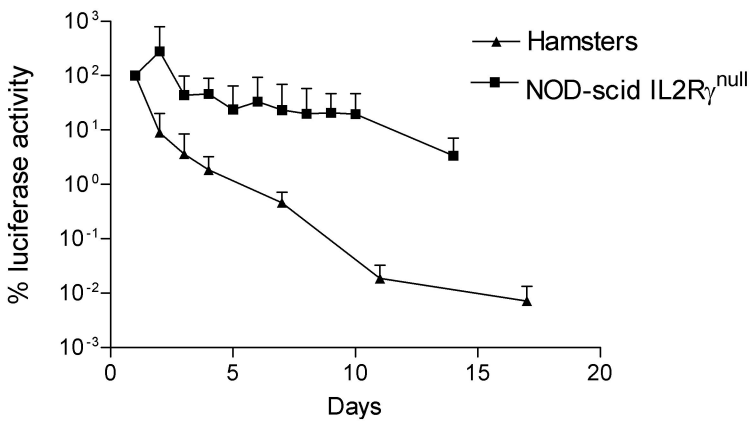
Hamsters
NOD-scid IL2Rγnull
% luciferase activity
Days